Journal of Pharmacological Sciences xxx (2014) 1–5

Contents lists available at ScienceDirect

Journal of Pharmacological Sciences

journal homepage: www.elsevier.com/locate/jphs

Short communication

Paroxetine prevented the down-regulation of astrocytic L-Glu transporters in neuroinflammation

Koki Fujimori [a, b], Junpei Takaki [a, b], Yukari Shigemoto-Mogami [a], Yuko Sekino [a], Takeshi Suzuki [b], Kaoru Sato [a, *]

[a] Laboratory of Neuropharmacology, Division of Pharmacology, National Institute of Health Sciences, 1-18-1 Kamiyoga, Setagaya-ku, Tokyo 158-8501, Japan
[b] Division of Basic Biological Science, Faculty of Pharmacy, Keio University, 1-5-30 Shiba-koen, Minato-ku, Tokyo 105-8512, Japan

ARTICLE INFO

Article history:
Received 4 August 2014
Received in revised form
26 August 2014
Accepted 18 September 2014
Available online xxx

Keywords:
Paroxetine
L-glutamate
Inflammation

ABSTRACT

The extracellular L-glutamate (L-Glu) concentration is elevated in neuroinflammation, thereby causing excitotoxicity. One of the mechanisms is down-regulation of astrocyte L-Glu transporters. Some antidepressants have anti-inflammatory effects. We therefore investigated effects of various antidepressants on the down-regulation of astrocyte L-Glu transporters in the in vitro neuroinflammation model. Among these antidepressants, only paroxetine was effective. We previously demonstrated that the down-regulation of astrocyte L-Glu transporters was caused by L-Glu released from activated microglia. We here clarified that only paroxetine inhibited L-Glu release from microglia. This is the novel action of paroxetine, which may bring advantages on the therapy of neuroinflammation.

Increasing evidence indicates that inflammatory processes play important roles in the pathogenesis of many neurodegenerative disorders (1–3). Under the neuroinflammatory conditions, it is known that the extracellular concentration of L-glutamate (L-Glu) and inflammatory mediators, such as proinflammatory cytokines, prostaglandins, free radicals and complements are elevated (4). L-Glu is one of the most abundant excitatory neurotransmitters in the mammalian CNS. The released L-Glu is immediately uptaken by astrocyte L-Glu transporters, GLAST (EAAT1 in human) and GLT-1 (EAAT2 in human), or sustained elevation of extracellular concentration of L-Glu induce excitotoxicity. The impairment of the astrocyte L-Glu transporters is reported in various neurological disorders including Alzheimer's disease (5), Parkinson's diseases (6) and amyotrophic lateral sclerosis (7). We found that the expression level of L-Glu transporters in astrocytes of astrocyte-microglia-neuron mixed culture was decreased in the *in vitro* model of the early stage of inflammation in the previous study (8). We clarified the interaction between astrocytes and microglia underlie the down-regulation of L-Glu transporters, i.e., activated microglia release L-Glu and the resulting elevation of extracellular L-Glu cause down-regulation of astrocytic L-Glu transporters. Some antidepressants are known to have anti-inflammatory effects (9, 10). In this study, therefore, we investigated the effects of various antidepressants on the decrease in the astrocytic L-Glu transporter function in the early stage of inflammation and the contribution of microglia to the effects.

Astrocyte-microglia-neuron mixed culture and microglia culture were performed according to the methods previously described (8). Antidepressants and serotonin (5-HT) were dissolved in PBS at 100 μM and 10 mM, respectively, and were diluted with culture medium at the time of use. At 8 DIV, the astrocyte-microglia-neuron mixed culture was treated with 10 ng/mL LPS for 72 h. Antidepressants were applied from 1 h before to the end of the LPS-treatment. Then the concentration of the L-Glu remaining in the culture medium 30 min after changing extracellular concentration of L-Glu to 100 μM was measured. The measurement of the extracellular L-Glu concentration in the medium was performed according to the methods previously described (8). Real-Time Quantitative RT-PCR, Western blotting, immunocytochemistry were also performed according to the methods previously

Abbreviations: ATP, adenosine 5′-triphosphate; CNS, central nervous system; DIV, days *in vitro*; GABA, γ-aminobutyric acid; L-glu, L-glutamate; LPS, lipopolysaccharide; PBS, phosphate-buffered saline; $P2X_4$, P2X prinoceptor 4; RNA, ribonucleic acid; SD, Sprague-Dawley; SDS, sodium dodecyl sulfate; SNRI, serotonin–norepinephrine reuptake inhibitor; SSRI, selective serotonin reuptake inhibitor; TCA, tricyclic antidepressant; 5-HT, 5-hydroxytryptamine.

* Corresponding author. Tel./fax: +81 3 3700 9698.
E-mail address: kasato@nihs.go.jp (K. Sato).

Peer review under responsibility of Japanese Pharmacological Society.

http://dx.doi.org/10.1016/j.jphs.2014.09.002

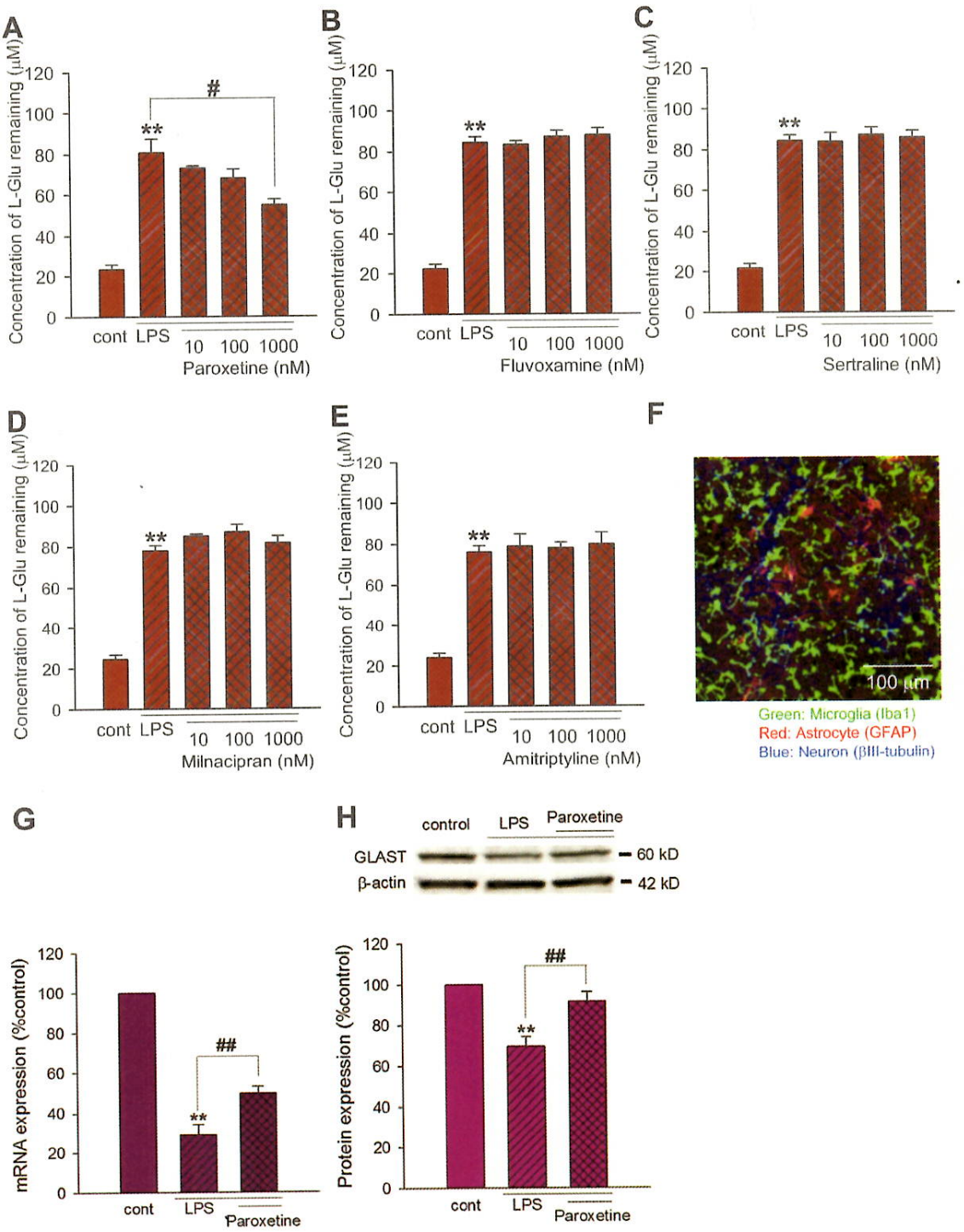

Fig. 1. Effects of antidepressants on the decreased L-Glu transport activity under the inflammatory condition. A–E. Antidepressants were applied to the mixed culture from 1 h before to the end of the LPS-treatment (10 ng/ml, 72 h). L-Glu transport activity was quantified as the L-Glu remaining 30 min after changing the extracellular concentration to 100 μM. Paroxetine prevented the LPS-induced decrease in the L-Glu transport activity in a concentration-dependent manner (A). Fluvoxamine (B), sertraline (C), milnacipran (D), and amitriptyline (E) had no effects. **: $p < 0.01$ vs. control group, #: $p < 0.05$ vs. LPS-treated group, Tukey's test following ANOVA ($N = 6$). F. Typical image of the microglia-astrocyte-neuron mixed culture immunostained with cell type-specific markers (Iba1: microglia; GFAP: astrocytes; βIII tubulin: neurons). G, H. Effects of paroxetine on the expression level of GLAST. Mixed cultures were treated with LPS (10 ng/ml) in the absence or presence of the paroxetine for 24 h (for mRNA level quantification) or 72 h (for protein level quantification). The expression level of GLAST was quantified at mRNA level (G) and protein level (H). LPS (10 ng/ml) caused significant decrease in GLAST mRNA level and paroxetine significantly prevented the decrease (G). LPS (10 ng/ml) caused significant decrease in GLAST protein level and paroxetine almost completely prevented the decrease (H). **: $p < 0.01$ vs. control group, ##: $p < 0.01$ vs. LPS-treated group, Tukey's test following ANOVA ($N = 5$).

Please cite this article in press as: Fujimori K, et al., Paroxetine prevented the down-regulation of astrocytic L-Glu transporters in neuroinflammation, Journal of Pharmacological Sciences (2014), http://dx.doi.org/10.1016/j.jphs.2014.09.002

described (8). The microglia culture was treated with LPS for 24 h in the presence or absence of antidepressants and the concentration of L-Glu in the medium was measured. All sets of the experiments were repeated in triplicate. All procedures described above were in accordance with institutional guidelines.

In the previous report, we showed that the expression level of astrocytic L-Glu transporters was decreased in the astrocyte-microglia-neuron mixed culture in LPS (10 ng/ml, 72 h)-induced inflammation model without cell death (8). We first compared the effects of various groups of antidepressants, i.e., selective serotonin reuptake inhibitors (SSRIs) (paroxetine, fluvoxamine, and sertraline), serotonin–norepinephrine reuptake inhibitor (SNRI) (milnacipran), and tricyclic antidepressant (TCA) (amitriptyline), on the decrease in the astrocytic L-Glu transporter function in this inflammation model. To quantify L-Glu transport activity, we measured the concentration of L-Glu remaining 30 min after changing the medium to the one containing 100 μM of L-Glu. In each set of experiment, LPS-induced decrease in the L-Glu transport activity was stably reproduced (Fig. 1A–E). Among antidepressants, only paroxetine prevented the LPS-induced decrease in L-Glu transport activity (Fig. 1A). The effect was concentration-dependent and reached significant at 1 μM. The other antidepressants had no effects (Fig. 1B–E). Typical image of the astrocyte-microglia-neuron mixed culture was shown in Fig. 1F. We have clarified that LPS-induced decrease in L-Glu transport activity was caused by the decrease in the expression level of GLAST, a predominant L-Glu transporter in the mixed culture, in both of mRNA and protein levels (8). In this study, LPS-induced decreases in the expression of GLAST, were reproduced at both of mRNA (28.8 ± 4.7% of the control) and protein (69.5 ± 4.7% of the control) levels (Fig. 1G, H). We then examined the effects of paroxetine on the LPS-induced decrease in the L-Glu transporter expression. Paroxetine significantly prevented the decreases at both of mRNA (28.8 ± 4.7 to 49.6 ± 3.3%; $n = 10$) and protein (from 69.5 ± 4.7% to 91.0 ± 5.1%; $n = 5$) levels (Fig. 1G, H). As is shown in Fig. 1, fluvoxamine and sertraline, the other SSRIs in this study, did not affect the decrease in L-Glu transport activity, suggesting that paroxetine revealed the effects through the mechanisms independent of its inhibitory effect on serotonin selective transporter. In support of this, LPS-induced decrease in L-Glu transport activity was not changed by the elevation of extracellular serotonin concentration (Fig. 2A). We also confirmed that paroxetine did not directly affect the L-Glu transport activity of the astrocyte culture (Fig. 2B). In our previous report, the down-regulation of GLAST in the inflammation model was caused by the elevation of extracellular L-Glu released from microglia (8). We therefore compared the effects of the antidepressants on LPS-induced L-Glu release from microglia. When microglia culture was treated with 10 ng/ml LPS for 24 h in the presence or absence of the antidepressants, only paroxetine suppressed L-Glu release in a concentration-dependent manner (Fig. 3A). The other antidepressants had no effects (Fig. 3B–E). We confirmed that paroxetine did not affect the microglial viability until 10 μM by LDH assay (data not shown). These results strongly suggest that the protective effect of paroxetine on the LPS-induced down-regulation of astrocytic L-Glu transporters was caused by the suppression of L-Glu release from microglia.

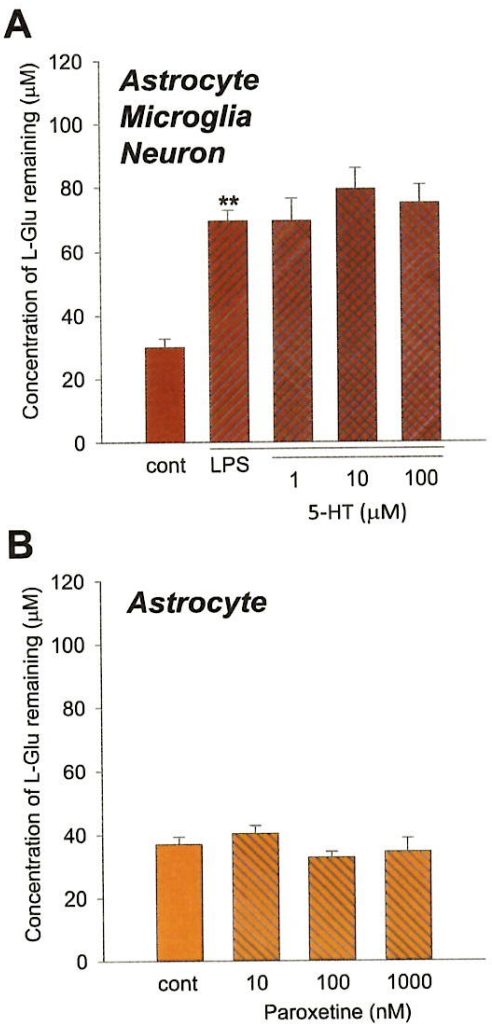

Fig. 2. Relation of the effects of paroxetine on LPS-induced decrease in L-Glu transport activity with its SSRI function and the direct effect on astrocytes. A. 72 h treatment with 5-HT (1–100 μM) did not affect LPS-induced decrease in the L-Glu transport activity. B. 72 h treatment with paroxetine (10–1000 nM) of astrocyte culture did not affect its L-Glu transport activity. **: $p < 0.01$ vs. control group, Tukey's test following ANOVA ($N = 6$).

The shape of microglia in the mixed culture was dramatically changed to amoeboid type by LPS and this morphological change was remarkably suppressed by paroxetine (unpublished observation). This suggests that paroxetine does not only suppress L-Glu release from microglia alone but also microglial activation. To demonstrate this possibility, the effect of paroxetine on the microglial activation is needed to be confirmed using multiple parameters. Because SSRIs have diverse chemical structures despite a common mode of action of 5-HT function (11), it is possible that paroxetine revealed the effects through interaction with paroxetine-specific target molecules. Because paroxetine exhibited the powerful inhibition of calcium influx via $P2X_4$ receptors (12), $P2X_4$ receptor is one of the most probable candidate molecules. The expression level of $P2X_4$ receptor in microglia is up-regulated in inflammatory pain model in spinal cord and is thought to be important for microglial inflammatory responses (13). MAPK signaling molecules (14) and GABA(B) receptor (15) are possibly involved in the paroxetine-specific effects as well. The effective concentration of paroxetine to reduce L-Glu release was 1 μM. According to the attached documents of paroxetine (http://www.info.pmda.go.jp/), intracerebral concentration of paroxetine reaches 77 nM by 25 mg/day-repeated administration. It is therefore unlikely that paroxetine affects astrocyte L-Glu transporters and microglia by the general dosage of SSRI. For clinical application of our present findings, further investigation concerning application period and dosage is needed.

Please cite this article in press as: Fujimori K, et al., Paroxetine prevented the down-regulation of astrocytic L-Glu transporters in neuroinflammation, Journal of Pharmacological Sciences (2014), http://dx.doi.org/10.1016/j.jphs.2014.09.002

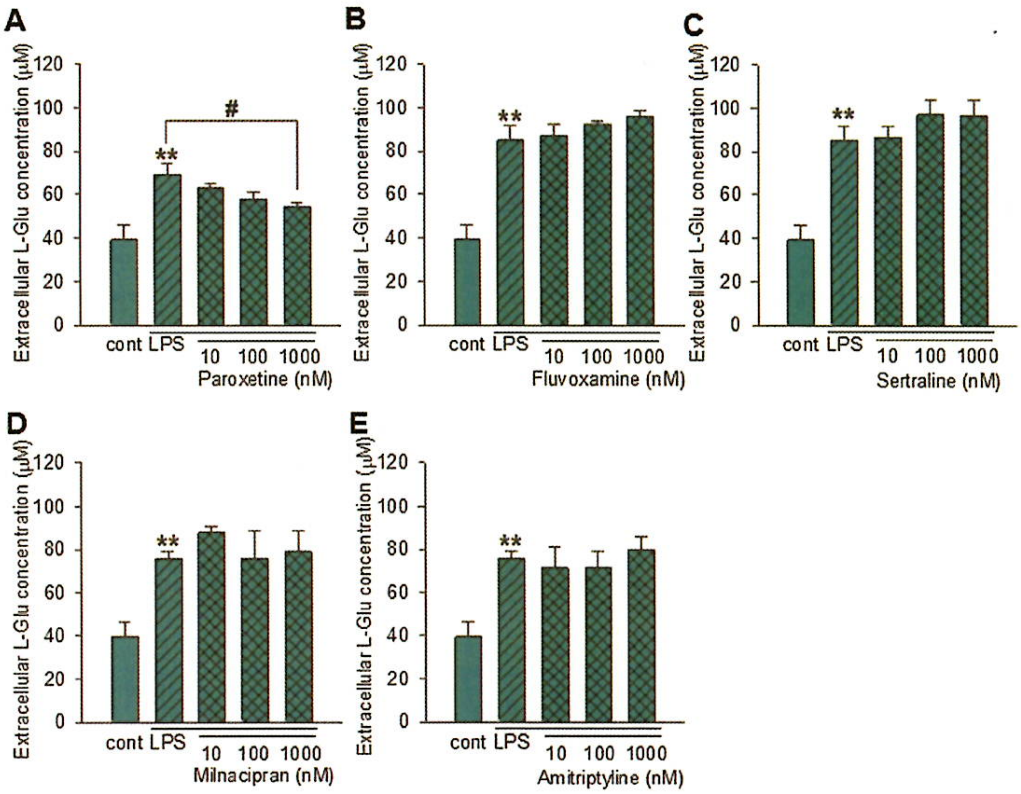

Fig. 3. Effects of antidepressants on the L-Glu release from microglia under the inflammatory condition. In each set of experiment, antidepressants were applied to the mixed culture from 1 h before to the end of the LPS-treatment (10 ng/ml, 24 h). The extracellular concentration of L-Glu was quantified. Paroxetine prevented the LPS-induced L-Glu release from microglia in a concentration-dependent manner (A). Fluvoxamine (B), sertraline (C), milnacipran (D), and amitriptyline (E) had no effects on LPS-induced L-Glu release from microglia. **: $p < 0.01$ vs. control group, #: $p < 0.05$ vs. LPS-treated group, Tukey's test following ANOVA ($N = 6$).

In conclusion, we found that paroxetine inhibit the L-Glu release from activated microglia and prevent down-regulation of astrocytic L-Glu transporters in the early stage of neuroinflammation. This is the novel pharmacological effect of paroxetine, which may bring advantages on the therapy of the disease associated with neuroinflammation.

Conflicts of interest

I declare that I have no significant competing financial, professional or personal interests that might have influenced the results and interpretation of the manuscript.

Author's contributions

K.F. performed experiments and manuscript writing.
J.T. performed experiments.
Y.S-M. provided advice on manuscript writing
Y.S. provided advice on manuscript writing
T.S. provided advice on the experimental direction and manuscript writing.
K.S. designed the experimental plan and performed experiments, manuscript writing.

Acknowledgments

This work was partly supported by a Grant-in-Aid for Young Scientists from Ministry of Education, Culture, Sports, Science, and Technology, Japan (KAKENHI 21700422), the Program for Promotion of Fundamental Studies in Health Sciences of National Institute of Biomedical Innovaton (10-21), Japan, a Health and Labor Science Research Grant for Research on Risks of Chemicals, a Labor Science Research Grant for Research on New Drug Development from the MHLW, Japan, awarded to K.S., Grant-in-Aid for research from MEXT, Japan (KAKENHI C23590113) awarded to T.S., and a Health and Labor Science Research Grant for Research on Publicly Essential Drugs and Medical Devices, Japan, awarded to Y.S.

References

(1) Bowerman M, Vincent T, Scamps F, Perrin FE, Camu W, Raoul C. Neuroimmunity dynamics and the development of therapeutic strategies for amyotrophic lateral sclerosis. Front Cell Neurosci. 2013;7:214.
(2) Liimatainen S, Lehtimaki K, Palmio J, Alapirtti T, Peltola J. Immunological perspectives of temporal lobe seizures. J Neuroimmunol. 2013;263:1–7.
(3) Schwartz M, Baruch K. The resolution of neuroinflammation in neurodegeneration: leukocyte recruitment via the choroid plexus. EMBO J. 2014;33:7–22.
(4) Lucas SM, Rothwell NJ, Gibson RM. The role of inflammation in CNS injury and disease. Br J Pharmacol. 2006;147(Suppl. 1):S232–S240.
(5) Masliah E, Alford M, DeTeresa R, Mallory M, Hansen L. Deficient glutamate transport is associated with neurodegeneration in Alzheimer's disease. Ann Neurol. 1996;40:759–766.
(6) Ferrarese C, Zoia C, Pecora N, Piolti R, Frigo M, Bianchi G, et al. Reduced platelet glutamate uptake in Parkinson's disease. J Neural Transm. 1999;106:685–692.
(7) Rothstein JD, Martin LJ, Kuncl RW. Decreased glutamate transport by the brain and spinal cord in amyotrophic lateral sclerosis. N Engl J Med. 1992;326:1464–1468.
(8) Takaki J, Fujimori K, Miura M, Suzuki T, Sekino Y, Sato K. L-glutamate released from activated microglia downregulates astrocytic L-glutamate transporter

Please cite this article in press as: Fujimori K, et al., Paroxetine prevented the down-regulation of astrocytic L-Glu transporters in neuroinflammation, Journal of Pharmacological Sciences (2014), http://dx.doi.org/10.1016/j.jphs.2014.09.002

expression in neuroinflammation: the 'collusion' hypothesis for increased extracellular L-glutamate concentration in neuroinflammation. J Neuroinflammation. 2012;9:275.
(9) Hashioka S, Klegeris A, Monji A, Kato T, Sawada M, McGeer PL, et al. Antidepressants inhibit interferon-gamma-induced microglial production of IL-6 and nitric oxide. Exp Neurol. 2007;206:33–42.
(10) Hwang J, Zheng LT, Ock J, Lee MG, Kim SH, Lee HW, et al. Inhibition of glial inflammatory activation and neurotoxicity by tricyclic antidepressants. Neuropharmacology. 2008;55:826–834.
(11) RJ B. Drugs and the treatment of psychiatric disorders. Goodman and Gilman's the pharmacological basis of therapeutics. In: Hardman JG, Limbird LE, Gilman AG, editors. 10th ed 2001. p. 447–483.
(12) Nagata K, Imai T, Yamashita T, Tsuda M, Tozaki-Saitoh H, Inoue K. Antidepressants inhibit P2X4 receptor function: a possible involvement in neuropathic pain relief. Mol Pain. 2009;5:20.
(13) Guo LH, Trautmann K, Schluesener HJ. Expression of P2X4 receptor by lesional activated microglia during formalin-induced inflammatory pain. J Neuroimmunol. 2005;163:120–127.
(14) Liu RP, Zou M, Wang JY, Zhu JJ, Lai JM, Zhou LL, et al. Paroxetine ameliorates lipopolysaccharide-induced microglia activation via differential regulation of MAPK signaling. J Neuroinflammation. 2014;11:47.
(15) Khundakar AA, Zetterstrom TS. Effects of GABAB ligands alone and in combination with paroxetine on hippocampal BDNF gene expression. Eur J Pharmacol. 2011;671:33–38.

Please cite this article in press as: Fujimori K, et al., Paroxetine prevented the down-regulation of astrocytic L-Glu transporters in neuroinflammation, Journal of Pharmacological Sciences (2014), http://dx.doi.org/10.1016/j.jphs.2014.09.002

Development/Plasticity/Repair

Microglia Enhance Neurogenesis and Oligodendrogenesis in the Early Postnatal Subventricular Zone

Yukari Shigemoto-Mogami,[1] Kazue Hoshikawa,[1] James E. Goldman,[2] Yuko Sekino,[1] and Kaoru Sato[1]

[1]Laboratory of Neuropharmacology, Division of Pharmacology, National Institute of Health Sciences, Tokyo 158-8501, Japan, and [2]Department of Pathology and Cell Biology, Columbia University College of Physicians and Surgeons, New York, New York 10032

Although microglia have long been considered as brain resident immune cells, increasing evidence suggests that they also have physiological roles in the development of the normal CNS. In this study, we found large numbers of activated microglia in the forebrain subventricular zone (SVZ) of the rat from P1 to P10. Pharmacological suppression of the activation, which produces a decrease in levels of a number of proinflammatory cytokines (i.e., IL-1β, IL-6, TNF-α, and IFN-γ) significantly inhibited neurogenesis and oligodendrogenesis in the SVZ. *In vitro* neurosphere assays reproduced the enhancement of neurogenesis and oligodendrogenesis by activated microglia and showed that the cytokines revealed the effects complementarily. These results suggest that activated microglia accumulate in the early postnatal SVZ and that they enhance neurogenesis and oligodendrogenesis via released cytokines.

Key words: **cytokine; microglia; neurogenesis; neurosphere; oligodendrogenesis; subventricular zone**

Introduction

CNS microglia have long been considered as resident immune cells, which are activated in response to pathological events. In pathological conditions, they change their morphology to an amoeboid shape, acquiring activation-specific phenotypes, such as chemotaxis, phagocytosis, and secretion of inflammatory cytokines (Nakajima and Kohsaka, 2001; Inoue, 2008; Monji et al., 2009; Kettenmann et al., 2011). However, microglia also have physiological roles in the normal CNS. They actively survey their territory with fine processes and receive stimuli from the environment as sensor cells (Kettenmann et al., 2011). *In vivo* lineage tracing studies have established that microglia differentiate from primitive myeloid progenitors that arise before embryonic day 8 and are identified in the CNS parenchyma even before definitive hematopoiesis (Ginhoux et al., 2010), whereas it has also been shown that microglia migrate from the lateral ventricle into the brain via the subventricular zone (SVZ) in the postnatal brain (Mohri et al., 2003). In the early embryonic brain, most microglia adopt an amoeboid morphology and characteristics of an activated form (Hirasawa et al., 2005). Microglia in the embryonic SVZ limit the production of cortical neurons by phagocytosing neural precursor cells (Cunningham et al., 2013). The number of microglia in the brain reaches a maximum during the early postnatal weeks (Wu et al., 1993; Xu and Ling, 1994), after which they transform into cells with a ramified shape, the typical morphology observed in the adult CNS (Ignácio et al., 2005). However, microglia are densely populated in neurogenic niches, such as the SVZ (Mosher et al., 2012), and appear more activated in the adult SVZ than in non-neurogenic zones (Goings et al., 2006). These developmental changes in the activation and the distribution of microglia strongly suggest that microglia play important roles in CNS development. However, the developmental dynamics of microglia in the postnatal SVZ and their roles in neurogenesis and gliogenesis at this stage are not well understood. We have examined the distribution and morphology of microglia in the rat forebrain during the neonatal-early postnatal period in detail and found a large number of active forms within the SVZ from P1 to P10, which then transformed from an activated form to a ramified form after P14. We here present evidence that microglia in the early postnatal SVZ promote both neurogenesis and oligodendrogenesis and that cytokines are important in these effects. To our knowledge, this is the first report showing a novel physiological function of microglia regulating neurogenesis and oligodendrogenesis in the early postnatal brain.

Materials and Methods

Animals and treatment. All animals were treated in accordance with the guidelines for the Care and Use of Laboratory Animals of the Animal Research Committee of the National Institute of Health Sciences and followed the *Guide for the Care and Use of Laboratory Animals*. All experiments were approved by the Animal Research Committee of National Institute of Health Sciences and conformed to the relevant regulatory standards. The Wistar rats were purchased from Japan SLC and maintained under specific pathogen-free conditions at a controlled temperature and humidity and on a 12 h light/12 h dark cycle and had *ad libitum*

Received April 15, 2013; revised Dec. 21, 2013; accepted Dec. 27, 2013.

Author contributions: K.S. designed research; Y.S.-M., K.H., and K.S. performed research; Y.S.-M., K.H., J.E.G., Y.S., and K.S. analyzed data; Y.S.-M., J.E.G., Y.S., and K.S. wrote the paper.

This work was supported in part by a Grant-in-Aid for Young Scientists from MEXT, Japan (KAKENHI 21700422), the Program for Promotion of Fundamental Studies in Health Sciences of NIBIO, Japan, a Health and Labor Science Research Grant for Research on Risks of Chemicals, a Labor Science Research Grant for Research on New Drug Development from the MHLW, Japan to K.S., and a Health and Labor Science Research Grant for Research on Publicly Essential Drugs and Medical Devices, Japan to Y.S.

The authors declare no competing financial interests.

This article is freely available online through the *J Neurosci* Author Open Choice option.

Correspondence should be addressed to Dr. Kaoru Sato, Laboratory of Neuropharmacology, Division of Pharmacology, National Institute of Health Sciences, Kamiyoga 1-18-1, Setagaya-ku, Tokyo 158-8501, Japan. E-mail: kasato@nihs.go.jp.

DOI:10.1523/JNEUROSCI.1619-13.2014

 0270-6474/14/342231-13$15.00/0

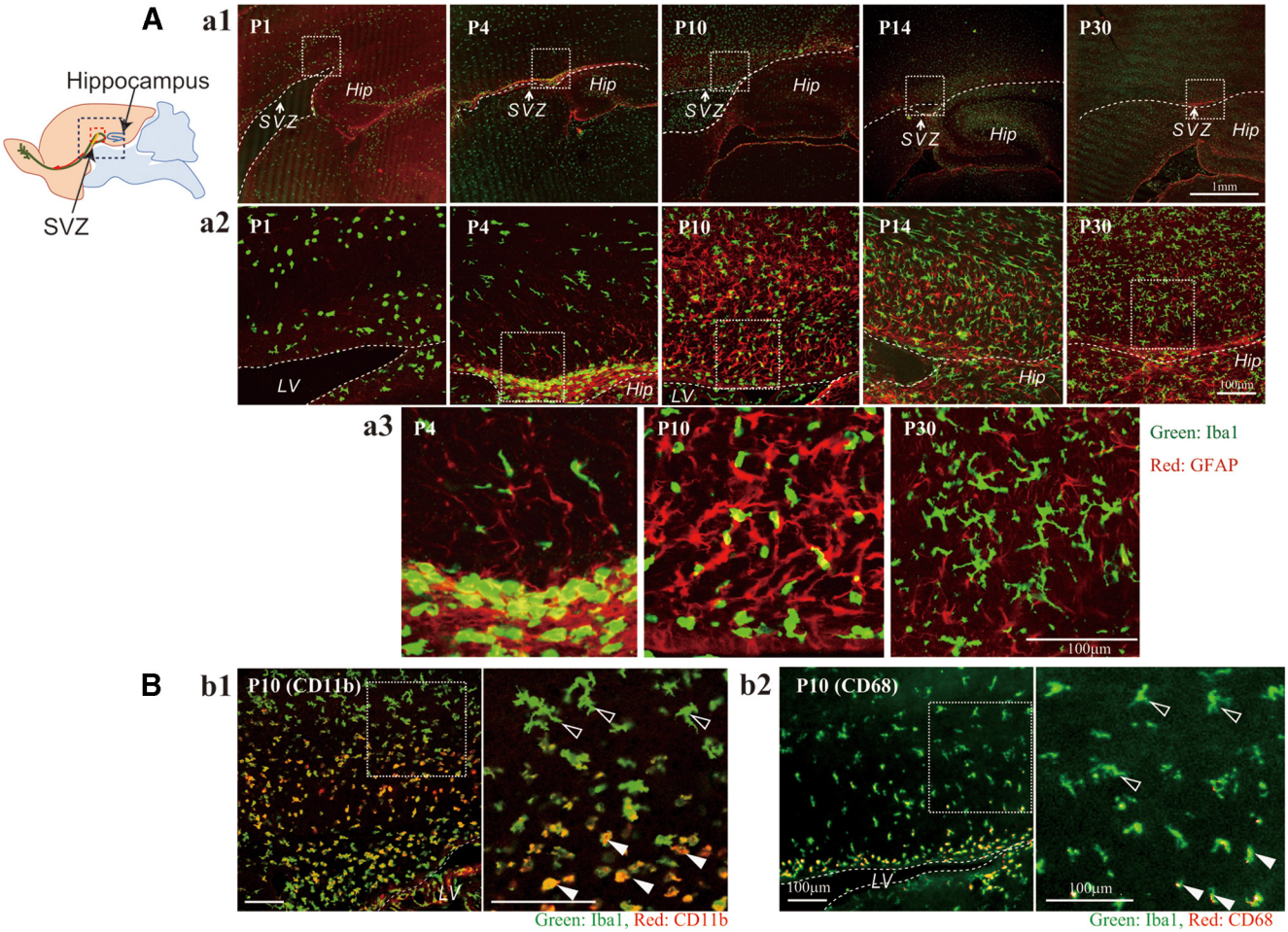

Figure 1. There is a population of activated microglia accumulated in the early postnatal SVZ. ***Aa1***, Distribution of microglia in the postnatal VZ/SVZ (P1, P4, P10, P14, P30). Sagittal sections of forebrains were immunostained with anti-Iba1 (green: microglia) and anti-GFAP antibodies (red: neural stem cells and astrocytes). ***Aa2***, Magnified images of the hatched squares in ***Aa1***. The accumulation in the SVZ in P4 and P10 was distinctive. ***Aa3***, Magnified images of the hatched squares in ***Aa2***. Morphological changes of microglia with age from amoeboid shape to more ramified shape is remarkable (P4, P10, P30). ***Bb1***, Activation of microglia in P10 SVZ. Sagittal sections immunostained with anti-CD11b (red: activated microglia) and anti-Iba1 antibodies (green: microglia). Right panel, Magnified image of the hatched square in the left panel. The microglia in the SVZ have an amoeboid shape and positive for CD11b (white arrowheads), whereas those outside SVZ have more ramified shape and are negative for CD11b (black arrowheads). ***Bb2***, Sagittal sections immunostained with anti-CD68 (red: activated microglia) and anti-Iba1 antibodies (green: microglia). Right panel, Magnified image of the hatched square in the left panel. The microglia in the SVZ have an amoeboid shape and positive for CD68 (white arrowheads), whereas those outside SVZ have more ramified shape and are negative for CD68 (black arrowheads). Similar results were obtained in three independent experiments.

access to food and water. Minocycline (30 mg/kg) or the same volume of PBS was injected into rats of either sex intraperitoneally for 3 d from postnatal day 2 (P2). Six hours after the last injection, rats were deeply anesthetized and the brains were removed on ice.

Immunohistochemistry (sagittal sections). Rats (P1, P4, P10, P14, P30) were anesthetized and then perfused with saline followed by 4% PFA, and then the brains were removed. From each half brain, sagittal sections were cut laterally at a thickness of 30 μm beginning 2 mm lateral from the midline. The sections were incubated for 2 h at room temperature in a blocking solution (3% normal goat serum, 0.3% Triton X-100 in PBS) and incubated for 24 h at 4°C in the solution, including the primary antibodies (rabbit anti-Iba1 antibody [019–9741, Wako; 1:500], mouse anti-GFAP antibody [MAB3402, Millipore; 1:200], mouse anti-rat CD11b antibody [MAB1405, AbD Serotec; 1:100], anti-rat CD68 antibody [MCA341R, AbD Serotec; 1:100], rabbit anti-Ki-67 [SP6, M3061, Spring Bioscience; 1:10], anti-nestin antibody [MAB353, Millipore; 1:100], goat anti-doublecortin [Dcx] antibody [sc-8066, Santa Cruz Biotechnology; 1:200], goat anti-PDGFRα antibody [sc-31178, Santa Cruz Biotechnology; 1:50], anti-oligodendrocyte marker O1 [O1] antibody [MAB344, Millipore, 1:50], mouse anti-MBP antibody [MAB 382, Millipore; 1:50], rabbit anti-ALDH1L1 antibody-astrocyte marker antibody [ab87117, Abcam; 1:1000], mouse anti-S100β antibody [S2532, Sigma; 1:100], rabbit anti IGF-1 antiserum [GroPep Biotechnology; [1:200]). After incubation, the sections were washed and incubated for 3 h at room temperature in the solution, including the secondary antibodies (anti-rabbit IgG-conjugated Alexa Fluorochrome or anti-mouse IgG-conjugated Alexa Fluorochrome [Invitrogen; 1:1000]). The stained sections were analyzed using a Nikon A1R-A1 confocal microscope system. To count the number of cells positive for each differentiation marker, 613 × 613 μm^2 and 1024 × 1024 μm^2 squares were set on both sides of the fornix. The cell numbers in the two squares were counted and averaged for the cell numbers in one section. The averaged data of 3 sections at 90 μm intervals were treated as the data of one animal and the data from 6 animals were statistically analyzed.

Immunohistochemistry (coronal sections). Three points on the skull at three different rostrocaudal stereotaxic coordinates (i.e., anterior, middle, posterior) were marked with animal tattoo ink (Ketchum) at P1. These three points with different rostrocaudal levels were determined according to a previous report (Suzuki and Goldman, 2003): rostral point: 2 mm anterior, 1 mm lateral to the bregma; middle point: 0.7 mm anterior, 1 mm lateral to the bregma; caudal point: 0.5 mm posterior, 1 mm lateral to the bregma. Then the animals were perfused at P1, P3, P10, and P30, and the brains were removed as described above. From each half brain, coronal sections were cut at each marked point from anterior to posterior. The sections were immunostained with anti-Iba1 and anti-CD68 as described above. After immunostaining, the sections were coun-

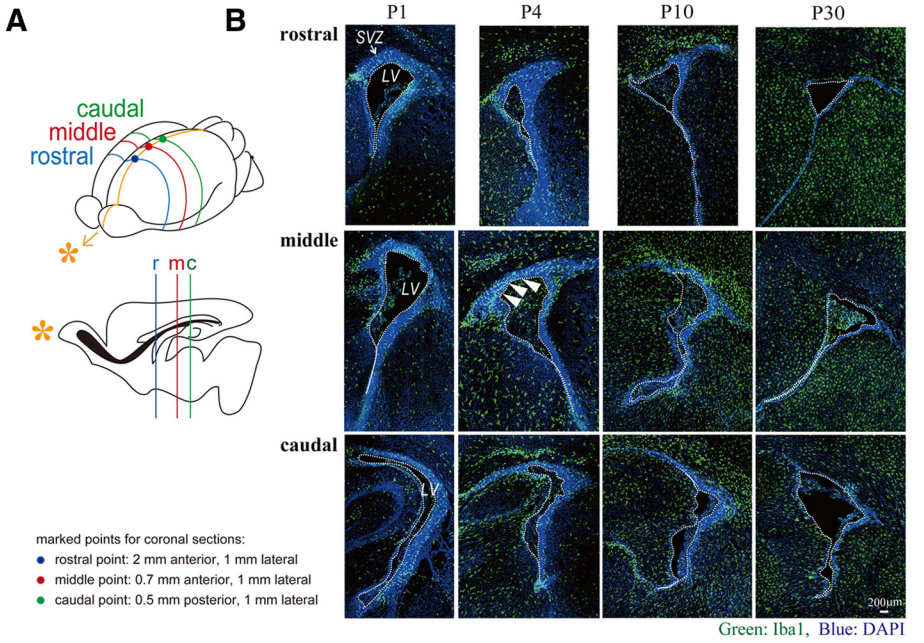
A
B
caudal
middle
rostral
r mc
P1
P4
P10
P30
rostral
middle
caudal
SVZ
LV
marked points for coronal sections:
rostral point: 2 mm anterior, 1 mm lateral
middle point: 0.7 mm anterior, 1 mm lateral
caudal point: 0.5 mm posterior, 1 mm lateral
200μm
Green: Iba1, Blue: DAPI

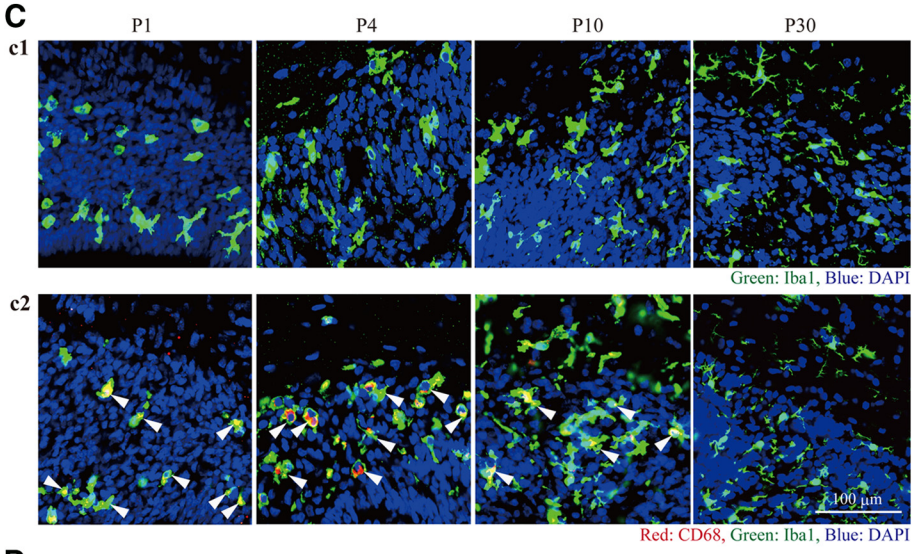
C
P1
P4
P10
P30
c1
Green: Iba1, Blue: DAPI
c2
100 μm
Red: CD68, Green: Iba1, Blue: DAPI

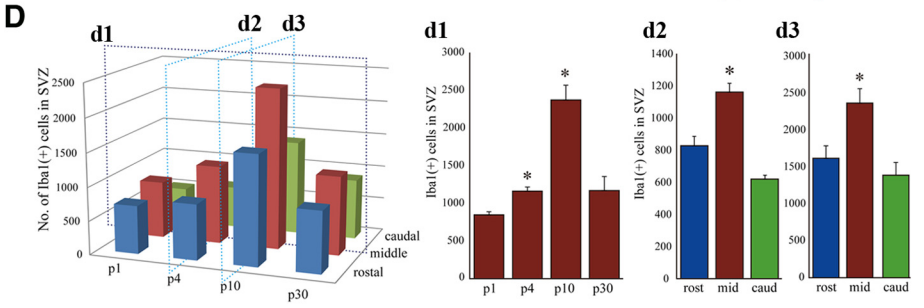
D
d1
d2
d3
No. of Iba1(+) cells in SVZ
caudal
middle
rostral
p1
p4
p10
p30
Iba1(+) cells in SVZ
rost
mid
caud

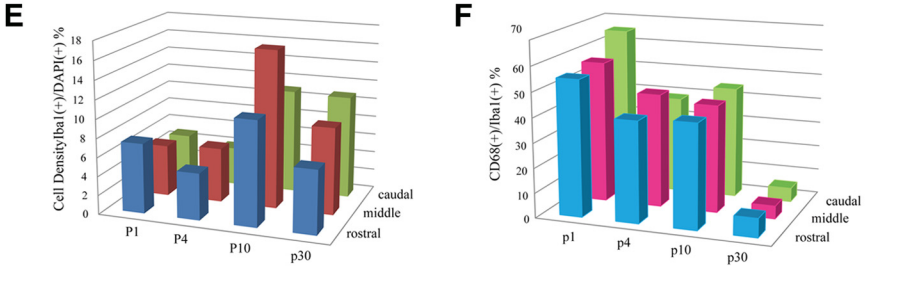
E
F
Cell DensityIba1(+)/DAPI(+) %
CD68(+)/Iba1(+) %
caudal
middle
rostral
P1
P4
P10
p30
p1
p4
p10
p30

terstained with DAPI (1:500; Invitrogen) for 30 min to visualize the SVZ. The cell numbers of microglia (Iba1$^+$) and activated microglia (Iba1$^+$ CD68$^+$) in the SVZ (the region with dense DAPI signals) were counted in one section. The averaged data of three sections at 90 μm intervals across the marked points were treated as the data for each rostrocaudal level. The data from 6 to 9 hemispheres per one rostrocaudal level were statistically analyzed.

Western blotting. P4 Wistar rat brains were cut into sagittal sections. Under a microscope, a parasagittal section (from 1 mm lateral, 2 mm thickness) was taken from each half brain and meninges were carefully removed. The VZ/SVZ was identified by its slightly darker, more transparent appearance compared with the overlying corpus callosum. We cut out the VZ/SVZ between 0.4 mm anterior and 3 mm posterior (posterior end of SVZ) from bregma so as not to include the rostral migratory stream. Dissected VZ/SVZ tissues were homogenized on ice in extraction buffer (20 mM Tris, 2 mM EDTA, 0.5 mM EGTA, 0.32 M sucrose, protease inhibitor mixture), and centrifuged at 1000 × *g* for 10 min. Proteins in the lysates were resolved with SDS-PAGE and transferred to PVDF membranes. The membranes were incubated overnight in BlockAce blocking solution at 4°C. Then the membranes were incubated with primary antibodies (anti-CD11b [1:1000], anti-CD68 [1:2000], anti-nestin [1:1000], anti-PDGFRα [1:200], anti-ALDH1L1 [1:1000], anti-S100β [1:2000]) for 1 h at 25°C. After washing three times, the membranes were incubated with HRP-conjugated anti-rabbit or anti-mouse antibody (1:5000) for 1 h at 25°C. The membranes were then washed three times and signals were visualized by chemiluminescence detectors LAS3000 (Fuji film).

Measurement of cytokine levels. Cytokine levels in the SVZ were determined with Bio-Plex cytokine analysis system (Bio-Rad Laboratories). Tissue lysates of VZ/SVZ fractions were obtained from rats at P1, P4, P10, and P30 as described in Western blotting. The concentrations of Il-1α, Il-1β, IL-2, IL-4, IL-6, Il-10, GM-CSF, IFN-γ, and TNF-α were measured by the Bio-Plex rat cytokine 9 plex kit according to the manufacturer's instruction. In some cases, IGF-1, Il-1β IL-6, TNF-α, and IFN-γ concentrations were measured by ELISA kit according to the manufacturer's instruction. The protein levels of tissue lysates were measured by BCA protein assay. The amount of each cytokine in 100 μg of total protein is shown for comparison. To determine the cytokine release from activated microglia *in vitro*, microglia were activated by LPS (10 ng/ml) in the presence or absence of minocycline (10 μM) for 30 min and washed carefully and incubated in the normal medium for 24 h. After 24 h incubation, the cell culture supernatants were collected, and concentration of Il-1β, IL-6, IFN-γ, and TNF-α were measured by ELISA kit.

Cell culture: neurosphere culture. Rat neural stem cells were cultured as previously described (Reynolds et al., 1992; Hamanoue et al., 2009) with slight modifications. Briefly, telencephalons were dissected from embryonic day 16 (E16) rats of either sex in ice-cold DMEM/F12, minced, and dispersed into single cells by pipetting. Cells were then cultured in DMEM/F12 containing B27 supplement (×200), 20 ng/ml FGF2, and 20 ng/ml EGF for 7 d. The primary neurospheres and single cells were differentiated in growth factor-free medium in glass chambers coated with ornithine/fibronectin. In some cases, primary neurosphere were incubated with TrypLE Select for 15 min and dissociated by pipetting. Single cells were differentiated in glass chambers coated with polyornithine/laminin.

Microglia culture. Rat microglia were cultured as previously described (Nakajima et al., 1992). In brief, mixed glial cultures were prepared from the cerebral cortex of P1 Wistar rats and maintained for 12–23 d in DMEM containing 10% FBS. The floating microglia over the mixed glial cultures were collected and transferred to appropriate dishes or transwells.

Neural stem cell differentiation assay. To examine the effects of activated microglia on neural development and the contribution of cytokines to the effects, we used modified cocultures of neurospheres with activated microglia. Microglia cultured independently of neurospheres on transwells were activated by LPS (10 ng/ml) in the presence or absence of minocycline (10 μM) for 30 min and washed carefully to prevent residual LPS and minocycline. The transwells on which microglia were cultured were set on the neurospheres 1 d after the starting point of the differentiation and incubated for differentiation periods suitable for neurons (7 d) or oligodendrocytes (11 d). In some cases, we performed the coculture of cells dissociated from neurospheres and activated microglia. To check the effects of minocycline alone, these cells were incubated in the presence of minocycline (10 μM) for 7 d. Neurospheres and single neural stem cells were immunohistochemically stained for β3-tubulin, PDGFRα, O4, GFAP, and TOTO3 according to the manufacture's instruction (Stem Cell Kits, R&D Systems). To examine the effects of function-blocking antibodies on differentiation, the neurospheres were differentiated in the presence of function-blocking antibodies (goat anti-rat IL-1β antibody [AF-501-NA, R&D Systems], goat anti-rat IL-6 antibody [AF-506, R&D Systems], TNF-α antibody [70R-TR007X, Fitzgerald], and goat anti-mouse/rat IFN-γ antibody [AF-585-NA, R&D Systems]) (1 μg/ml for each). The effects of these function-blocking antibodies were compared with the same concentration of isotype-matched control IgG: normal goat IgG control [AB-108-C, R&D Systems] and rabbit IgG control [31R-AR001, R&D Systems] (1 μg/ml for each). The effect of the mixture of function blocking antibodies (goat anti-rat IL-1β antibody, goat anti-rat IL-6 antibody, TNF-α antibody, and goat anti-mouse/rat IFN-γ antibody, 1 μg/ml for each) was compared with the control, which included same concentrations of isotype-matched control IgGs (i.e., 3 μg/ml of normal goat IgG control and 1 μg/ml of rabbit IgG control). To examine the effects of a single cytokine, the neurospheres were differentiated in the presence of each individual recombinant cytokine (rIL-1β, rIL-6, rTNF-α, and rIFN-γ at 1 or 10 ng/ml). After the differentiation period, the cells were stained immunocytochemically as described above.

Data analysis and statistics. All data are shown as the mean ± SEM. Statistical analysis was performed using Student's *t* test, or Tukey's test by ANOVA. Differences were considered to be significant at $p < 0.05$.

Materials. Minocycline, LPS, anti-S100β antibody (S2532), and EGF were purchased from Sigma. Bio-Plex rat cytokine 9 plex was purchased from Bio-Rad Laboratories. Recombinant cytokines (rIL-1β, rIL-4, rIL-6, rIFN-γ, rTNF-α) and FGF2 were purchased from PeproTech. Maximum sensitivity substrate and BCA protein assay were purchased from Thermo Scientific. CanGet Signals was purchased from Toyobo. HRP-conjugated anti-rabbit, mouse antibodies were purchased from GE Healthcare Life Science. DAPI, TOTO3, anti-mouse, sheep, rabbit IgG, and anti-mouse IgM-conjugated AlexaFluor were purchased from Invitrogen. BlockAce was purchased from DS Pharma Biomedical. B27 supplement, TrypLE Serect, FBS, and DMEM were purchased from Invitrogen.

Results

We first investigated the distribution of microglia in the postnatal rat forebrain (Figs. 1 and 2). Sagittal sections were immuno-

←

Figure 2. The temporal and spatial dynamics of activated microglia in the postnatal SVZ. ***A***, A schematic of the rostrocaudal levels in this experiment. ***B***, The distribution of microglia in the rostral, medial, and caudal SVZ at P1, P4, P10, and P30. Coronal sections of forebrains at rostral (2 mm anterior to the bregma), medial (0.7 mm anterior to the bregma), and caudal (0.5 mm posterior to the bregma) levels were immunostained with anti-Iba1 (green: microglia) followed by DAPI staining (blue: cell nuclei). A population of activated microglia accumulated within the SVZ at P1-P10. ***Cc1***, Typical morphology of microglia in the middle SVZ at P1, P4, P10, and P30. Morphological change of microglia with age from amoeboid shape to more ramified shape is remarkable. ***Cc2***, The middle SVZ sections immunostained with anti-CD68 (red: activated microglia) and anti-Iba1 antibodies (green: microglia). The microglia at P1, P4, and P10 in the SVZ have an amoeboid shape and are positive for CD68 (representative cells: white arrowheads), whereas those at p30 have a more ramified shape and are negative for CD68. ***D***, The quantification of the number of Iba1$^+$ cells in the SVZ. ***d1***, Time course of the Iba1$^+$ microglia in the middle SVZ. The number peaked at P10. d2, d3, The comparison of the numbers of microglia among the rostral, middle, and caudal SVZ at P4 (***d2***) and P10 (***d3***). *$p < 0.05$ versus p1 or rost group (Tukey's test by ANOVA). Data are mean ± SEM. ***E***, The cell density of Iba1$^+$ microglia at different rostrocaudal levels at P1, P4, P10, and P30. The cell density of microglia in the SVZ paralleled with that of the number of microglia throughout a period of the observation. ***F***, The ratio of activated microglia in the SVZ (CD68$^+$/Iba1$^+$). During the experimental period, the highest ratio was obtained at P1. We confirmed the similar results in three independent experiments.

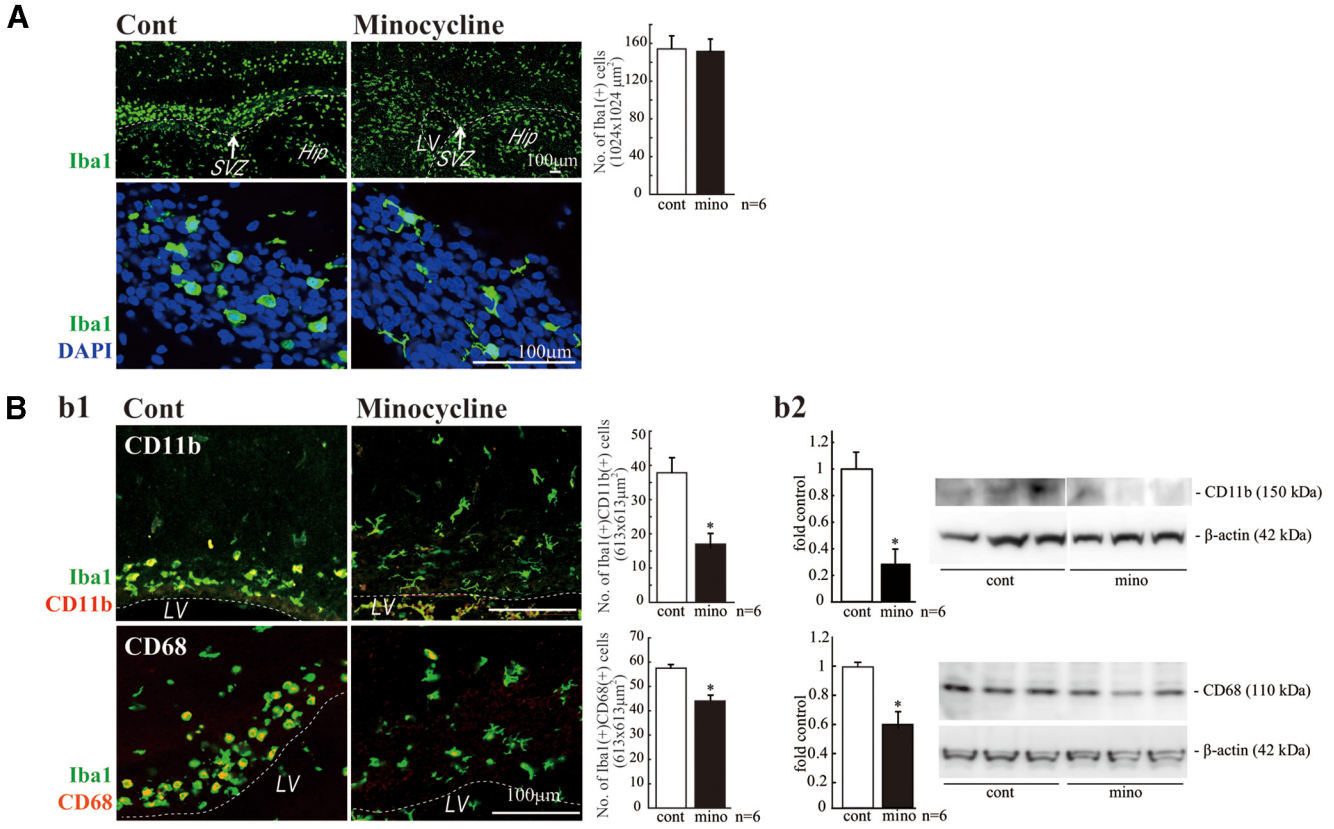

Figure 3. Minocycline suppressed microglial activation *in vivo*. ***A***, Effects of minocycline on the number of Iba1$^+$ cells in the SVZ and their morphologies. Minocycline was administered by intraperitoneal injection for 3 d beginning at P2 (30 mg/kg/d, P2-P4, $n = 6$/group). Sagittal sections of minocycline-treated forebrains were immunostained for Iba1 (green) followed by DAPI staining (cyan). Although the number of Iba1$^+$ microglia in the SVZ did not change (graph), their shape shifted from an amoeboid type to a more ramified type by minocycline (bottom). ***Bb1***, Effects of minocycline on the expression of activation markers and the morphologies of microglia. Sagittal sections of minocycline-treated forebrains were immunostained for Iba1 (green), and CD11b (red), and CD68 (red). Minocycline significantly decreased the number of cells positive for CD11b or CD68. The morphologies of the cells were also changed from amoeboid shape to more ramified shape. ***Bb2***, The significant decrease in the expression of CD11b and CD68 was confirmed by Western blotting of the SVZ as well. *$p < 0.05$ (Student's t test). Data are mean ± SEM. Similar results were obtained in three independent experiments.

stained with anti-Iba1, the marker for all microglia (green: microglia), and anti-GFAP antibodies (red: neural stem cells and astrocytes) at P1, P4, P10, P14, and P30. We found that a large number of microglia accumulated in the postnatal SVZ from P1 to P10 (Fig. 1*A*), especially at P4. The microglia in the VZ/SVZ at P1 and P4 display an amoeboid shape, whereas those outside the SVZ have a more ramified shape (Fig. 1*Aa2*). At P10, the number of microglia outside the SVZ had dramatically increased; the microglia in the VZ/SVZ remained amoeboid. At P14, the number of microglia had increased further and now ramified microglia were also observed in the VZ/SVZ. At P30, the numbers of microglia in the SVZ had decreased and most of the microglia had assumed a ramified shape. Further magnified images in Figure 1*Aa3* show that the shape of microglia in the SVZ changed gradually from amoeboid (P4) to ramified (P30). Figure 1*B* shows the expression of CD11b (Fig. 1*Bb1*) and CD68 (Fig. 1*Bb2*) in the SVZ microglia at P10. CD11b is potentially a marker for all microglia; however, its level is highly elevated by activation. CD68 is a marker for activated microglia. The levels of CD11b and CD68 are much higher in the amoeboid microglia in the SVZ (white arrowheads) than in the ramified ones outside the SVZ (black arrowheads), indicating that the SVZ amoeboid microglia have an activated phenotype.

To examine the developmental dynamics of microglia in the SVZ temporally and spatially, we examined the distribution of microglia in coronal sections that include rostral, medial, and caudal SVZ at P1, P4, P10, and P30 (Fig. 2). Each rostrocaudal level was determined according to a previous report (Suzuki and Goldman, 2003). Coronal sections were immunostained with anti-Iba1 (green: microglia) followed by DAPI staining (blue: cell nuclei) (Fig. 2*B*,*C*). The SVZ could be clearly delineated by its dense cellularity. From P1 to P10, a large number of microglia accumulated at all rostral, middle, and caudal levels. When we quantified the number of microglia in the SVZ, they gradually increased from P1 to P10, reached a maximum at p10, and decreased at P30 at all coronal levels (Fig. 2*B*,*D*, d1). Microglia displayed an amoeboid shape at P1, P4, and P10 but had become more ramified at P30 (Fig. 2*Cc1*). Among the different rostrocaudal levels, the number of microglia in the middle SVZ was significantly larger than in other levels at all ages (Fig. 2*D*, d2, d3). The changes in cell density (i.e., the ratio of Iba1$^+$/DAPI$^+$) of microglia in the SVZ paralleled that of the number of microglia throughout the period of observation (Fig. 2*E*). We next examined immunostaining for CD68 in SVZ microglia. Figure 2*Cc2* shows representative images of double staining with anti-Iba1 and anti-CD68. At P1 and P4, most Iba1+ microglia in the SVZ were also positive for CD68. At P4, the CD68 signals became much stronger. At P10, a few microglia had appeared that had little CD68. At P30, double-positive cells were markedly decreased in number. The time course of the ratio of CD68$^+$/Iba1$^+$ cells is shown in Figure 2*F*: the highest ratio was obtained at P1. The ratios at P4 and P10 were almost equivalent and then were

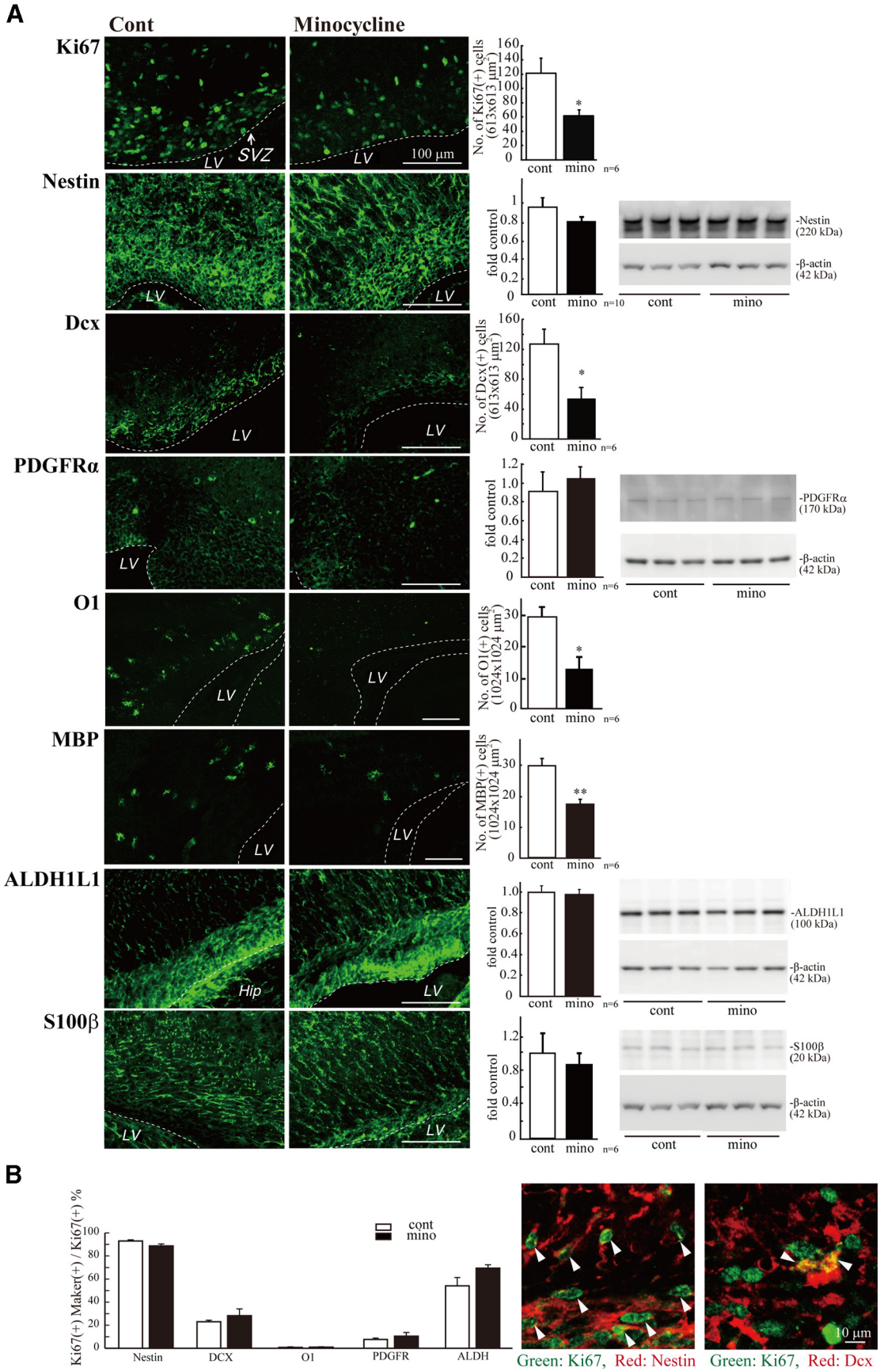

Figure 4. Minocycline decreased the numbers of proliferating cells, neuronal progenitors, and oligodendrocyte progenitors in the early postnatal SVZ. ***A***, Minocycline was administered by intraperitoneal injection for 3 d beginning at P2 (30 mg/kg/d, P2-P4, $n = 6$/group). Sagittal sections of forebrains were immunostained with antibodies to Ki67, nestin, Dcx, PDGFRα, O1, MBP, ALDH1L1, and S100β. The numbers of cells positive for Ki67, Dcx, MBP, or O1 were counted, whereas the protein levels of nestin, PDGFRα, ALDH1L1, and S100β (*Figure legend continues*.)

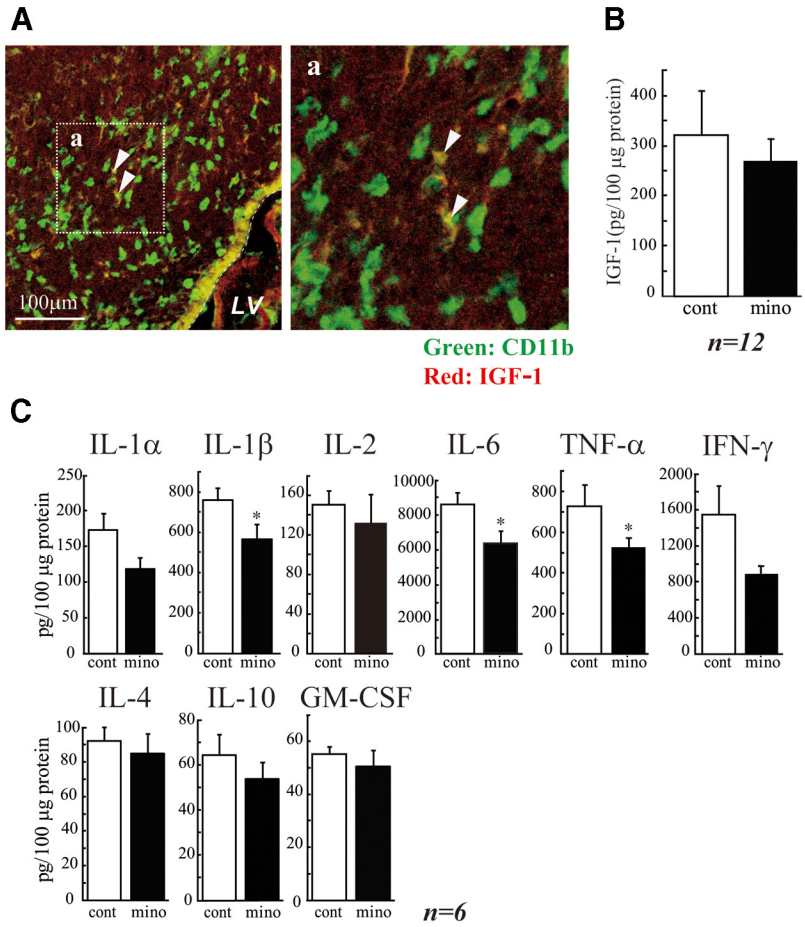

Figure 5. The activated microglia raised the cytokine levels in the SVZ. ***A***, A subpopulation of the microglia express IGF-1 in the early postnatal SVZ, but IGF-1 is not involved in the action of activated microglia during this period. Sagittal sections were immunostained with anti-CD11b (green: microglia) and anti IGF-1 (red) antibodies. Right panel, Magnified image of the square in the left. A subpopulation of microglia is positive for IGF-1 (arrowheads). The percentage of CD11b $^+$IGF-1 $^+$ was 43.42 ± 6.72% in CD11b $^+$ cells. ***B***, Minocycline did not affect the amount of IGF-1 in the early postnatal SVZ. Minocycline was administered by intraperitoneal injection for 3 d beginning at P2 (30 mg/kg/d, P2-P4, $n = 6$/group), and the amount of IGF-1 in the SVZ was quantified by ELISA. ***C***, Minocycline decreased the amount of inflammatory cytokines in the SVZ. IL-1α, IL-1β, IL-2, IL-4, IL-6, IL-10, GM-CSF, IFN-γ, and TNF-α levels in the SVZ tissue lysate were measured by BioPlex cytokine detection assay system. $^*p < 0.05$ (Student's t test). $n = 6$ rats/group. Data are mean ± SEM. Similar results were obtained in two independent experiments.

remarkably decreased at P30. These results are consistent with those obtained from the sagittal sections (Fig. 1), showing the population of activated microglia that accumulated within the SVZ during the early postnatal period.

We therefore examined the specific roles of these microglia in the early postnatal SVZ. At early postnatal ages, both neurogenesis and gliogenesis are active in the SVZ (Gould et al., 1999; Wagner et al., 1999; Doetsch and Scharff, 2001; Zerlin et al., 2004; Marshall et al., 2008). To suppress the activation of microglia, we used minocycline, a tetracycline antibiotic, long used to suppress microglial activation (Tikka et al., 2001; Zhao et al., 2007). We first verified the effects of minocycline on the activation of microglia. Minocycline was administered by intraperitoneal injection for 3 d beginning at P2 (30 mg/kg/d, P2-P4, $n = 6$/group), and sagittal sections of minocycline-treated rat forebrains were immunostained for Iba1, CD11b, and CD68. Minocycline did not change the numbers of Iba1-positive microglia in the VZ/SVZ (Fig. 3*A*, top), but it dramatically changed their shape from amoeboid to more ramified (Fig. 3*A*, bottom). The number of CD11b $^+$ cells was significantly decreased (Fig. 3*Bb1*, top and graph), and the decrease in CD11b levels in the SVZ was confirmed by Western blotting (Fig. 3*Bb2*, top graph and photo). The number of CD68 $^+$ cells and the level of CD68 were also decreased (Fig. 3*B*, bottom data). These results indicate that our administration of minocycline suppresses the activation of SVZ microglia.

We then investigated the effects of minocycline on early postnatal differentiation. After the administration of minocycline, sagittal sections were immunostained with differentiation markers: Ki67 (proliferating cells), nestin (stem cells), Dcx (neuronal progenitors), PDGFRα (oligodendrocyte progenitors [polydendrocytes]), O1 (oligodendrocyte progenitors [premyelinating oligodendrocytes]), MBP (mature oligodendrocyte [premyelinating and myelinating oligodendrocytes] (Nishiyama et al., 2009), ALDH1L1 (astrocyte progenitors), and S100β $^+$ (astrocytes) (Fig. 4*A*). The numbers of cells positive for Ki67, Dcx, O1, and MBP were counted, whereas the levels of nestin, PDGFα, ALDH1L1, and S100β were examined by Western blotting because it was hard to discriminate the cell morphologies by these signals. Minocycline significantly decreased the number of Ki67 $^+$ cells and slightly decreased the level of nestin. The number of cells positive for Dcx was also significantly reduced. Furthermore, minocycline decreased the numbers of cells positive for O1 and MBP, whereas the numbers of PDGFRα $^+$ cells rather tended to increase. The levels of ALDH1L1 and S100β did not change. These results suggest that activated microglia in the early postnatal SVZ enhance neurogenesis and oligodendrogenesis, and activated microglia affect oligodendrocyte progenitors at rather later stage of differentiation. We also performed the double staining of Ki67 with the respective differentiation markers (Fig. 4*B*). Although the total number of Ki67 $^+$ cells was decreased by minocycline, consistent with Figure 4*A*, the percentage of Ki67 $^+$ cells also positive for the respective differentiation markers did not change in the absence or presence of minocycline (Fig. 4*B*, left graph), suggesting that minocycline did not affect the proliferation of progenitors of the specific cell types. Typical images of the SVZ cells positive for

←

(*Figure legend continued.*) were examined by Western blotting. Minocycline significantly decreased the number of Ki67 $^+$ proliferating cells and decreased the level of nestin. The number of cells positive for Dcx was significantly reduced. Minocycline decreased the numbers of cells positive for O1 and MBP, whereas the expression level of PDGFRα tended to increase. $^*p < 0.05$, $^{**}p < 0.01$ (Student's t test). $n = 6$ mice/group. Data are mean ± SEM. ***B***, The ratio of the Ki67 $^+$ cells also positive for respective differentiation markers did not change in the absence or presence of minocycline (left graph). Typical images of the cells positive for Ki67 and Nestin, and the cells positive for Ki67 and Dcx in the control group are shown (right panels). We confirmed the same results in three independent experiments.

Ki67 and Nestin, and the cells positive for Ki67 and Dcx in the control group are shown (Fig. 4*B*, right panels).

Butovsky et al. (2006a) have reported that IGF-1 released from activated microglia promoted neurogenesis and oligodendrogenesis from adult stem/progenitor cells. We examined whether microglia in the early postnatal SVZ produce IGF-1 (Fig. 5*A*). Microglia did contain IGF-1 protein, but the percentage of CD11b$^+$ cells also positive for IGF-1$^+$ was 43.42 ± 6.72%. Furthermore, the amount of IGF-1 in the SVZ tissue lysates was not decreased by minocycline (Fig. 5*B*). These results suggest that, although a fraction of activated microglia in the early postnatal SVZ did produce IGF-1, the effects of activated microglia on neurogenesis and oligodendrogenesis obtained in our study were independent of IGF-1. Activated microglia release a number of cytokines. In some cases other than pathological conditions, cytokines also have physiological roles (Schäfers and Sorkin, 2008; Spedding and Gressens, 2008; Camacho-Arroyo et al., 2009; Miller et al., 2009; Spooren et al., 2011). We therefore investigated whether the SVZ microglia cause the increase in cytokine concentrations in the early postnatal SVZ (Fig. 5*C*). We examined the effects of minocycline on the levels of IL-1α, IL-1β, IL-2, IL-4, IL-6, IL-10, GM-CSF, IFN-γ, and TNF-α. To measure multiple cytokines in a small volume of tissue samples simultaneously, we used the BioPlex cytokine detection assay system (Bio-Rad). The levels of IL-1β, IL-6, and TNF-α were significantly decreased by the 3-day intraperitoneal administration of minocycline (Fig. 5*C*). Although the difference was not significant, the level of IFN-γ also tended to be decreased.

To examine more directly whether these cytokines affected neurogenesis and oligodendrogenesis, we performed *in vitro* experiments, coculturing neural stem cells with activated microglia. Microglia cultured independently of neurospheres on transwells were activated by LPS (10 ng/ml, 30 min) in the presence or absence of minocycline (10 μM). The microglia were carefully washed to remove residual LPS and minocycline, and then the transwell on which microglia were cultured was set onto the neurosphere cultures in prodifferentiation conditions. The activated microglia significantly increased the number of β3-tubulin$^+$ and O4$^+$ cells but had no effects on GFAP$^+$ cells in neurospheres (Fig. 6*A*,*B*). Minocycline almost completely suppressed the effects of activated microglia on the numbers of cells positive

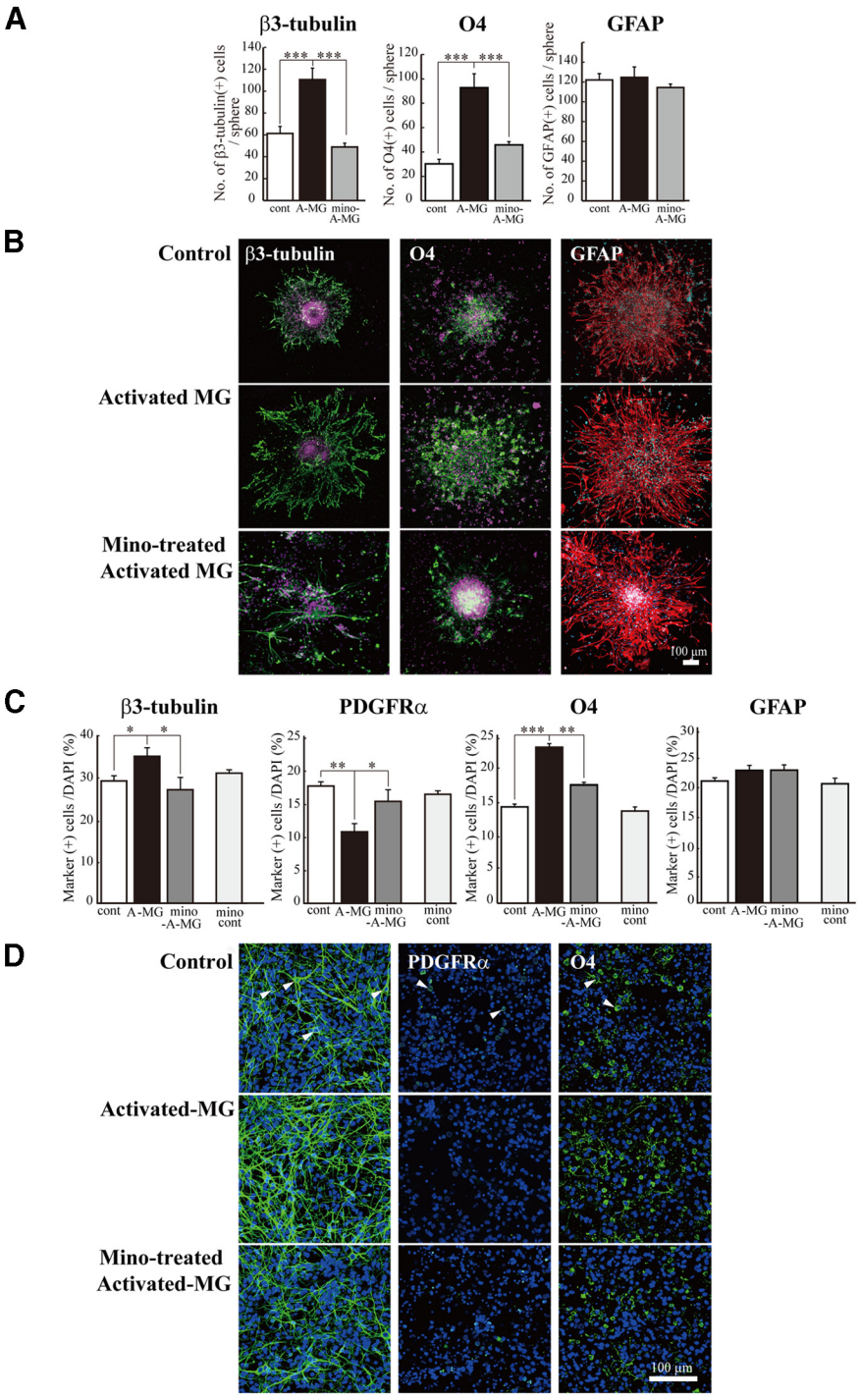

Figure 6. The reproduction of the enhancement of neurogenesis and oligodendrogenesis by activated microglia *in vitro*. Microglia cultured independently of neurosphere on transwells were activated by LPS (10 ng/ml, 30 min) in the presence or absence of minocycline (10 μM), washed carefully, and the transwells were set onto the neurospheres or dissociated cells from neurosphere in prodifferentiation conditions. After differentiation periods suitable for neurons (7 d) or oligodendrocytes (11 d), neurospheres were stained for β3-tubulin (green), PDGFRα (green), O4 (green), GFAP (red), and TOTO3 (cyan). To check the effects of minocycline alone, dissociated cells were incubated in the presence of minocycline (10 μM) for 7 d. ***A***, Quantification of the numbers of neurons, oligodendrocyte progenitors, or astrocytes differentiated from neurospheres cocultured with activated microglia in the presence or absence of minocycline. ***$p < 0.001$ (Tukey's test by ANOVA). $n = 12$ neurospheres/group. Data are mean ± SEM. ***B***, Representative immunostained images of neurospheres cocultured with activated microglia in the presence or absence of minocycline. ***C***, The effects of activated microglia on differentiation of single cells dissociated from neurospheres in the presence or absence of minocycline. The effects of minocycline alone were also shown (mino-cont in each graph). *$p < 0.05$, **$p < 0.01$, ***$p < 0.001$. (Tukey's test by ANOVA). $n = 12$ neurospheres/group. Data are mean ± SEM. ***D***, Images of cells immunostained for differentiation markers. Arrowheads indicate the representative cells positive for the differentiation markers.

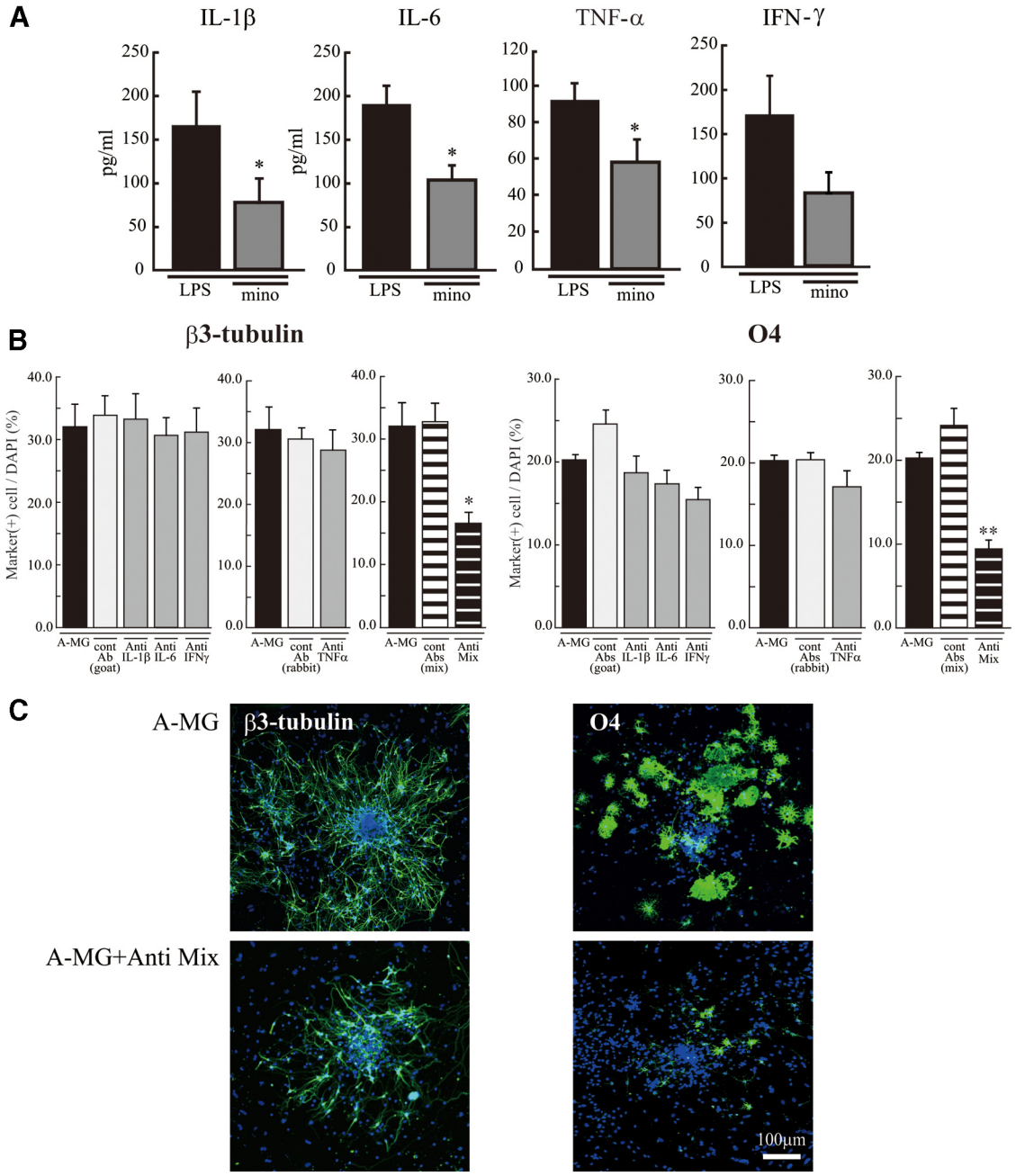

Figure 7. The *in vitro* enhancement of neurogenesis and oligodendrogenesis by activated microglia was suppressed by the mixture of function-blocking antibodies (anti-IL-1β, anti-IL-6, anti-TNF-α, and anti-IFN-γ). ***A***, The release of IL-1β, IL-6, TNF-α, or IFN-γ from activated microglia was suppressed by minocycline. Cultured microglia were activated by LPS (10 ng/ml, 30 min) in the absence and presence of minocycline (10 μM). The concentration of each cytokine in the supernatant was measured by ELISA 24 h after. *$p < 0.05$ (Student's *t* test). Data are mean ± SEM. ***B***, Effects of function-blocking antibodies to IL-1β, IL-6, TNF-α, and IFN-γ on enhanced neurogenesis and oligodendrogenesis by the activated microglia. The neurospheres were differentiated in the absence or presence of functional blocking antibodies (goat anti-rat IL-1β antibody, goat anti-rat IL-6 antibody, TNF-α antibody, or goat anti-mouse/rat IFN-γ antibody) (1 μg/ml for each) and a mixture of all of these antibodies. After a differentiation period suitable for neurons (7 d) or oligodendrocytes (11 d), neurospheres were stained for β3-tubulin (green), O4 (green), and TOTO3 (cyan). The data of single function blocking antibodies were compared with the controls, which include the same concentration of isotype-matched control IgGs (1 μg/ml for each). The data of the mixture of function blocking antibodies were compared with the controls, which include the same concentrations of isotype-matched control IgGs (i.e., 3 μg/ml of normal goat IgG control and 1 μg/ml of rabbit IgG control). *$p < 0.05$. **$p < 0.01$, versus isotype-matched control IgG group (Tukey's test by ANOVA). Data are mean ± SEM. ***C***, Representative immunostained images of neurospheres cocultured with activated microglia in the absence or presence of the mixture of the function-blocking antibodies. We confirmed the same results in three independent experiments.

for β3-tubulin or O4. We further confirmed these results using a differentiation assay with cells dissociated from neurospheres (Fig. 6*C*,*D*). With this protocol, the morphology of each cell could be discriminated more clearly. Consistent with the results described above, an increase in the numbers of cells positive for β3-tubulin and O4 was induced by activated microglia (Fig. 6*C*,*D*). Of note, PDGFRα^+ cells were decreased by activated microglia, whereas O4$^+$ cells were increased by activated microglia. Minocycline suppressed both of these effects, suggesting that activated microglia affect the later stage of oligodendrogenesis, thereby reducing the size of PDGFα^+ progenitor pool. In this experiment, we also checked the effects of minocycline alone (10 μM) on neurogenesis and oligodendrogenesis (Fig. 6*C*, "mino-cont" in each graph). Minocycline did not affect the numbers of